Experimental Study on Shear Strength of Saturated Remolded Loess

Jie Lai
Xi'an Research Institute of High Technology: PLA Rocket Force University of Engineering
Liu Yun
Xi'an Research Institute of High Technology: PLA Rocket Force University of Engineering
Yuzhou Xiang
Chongqing Chengtou Road and Bridge Administration
Wei Wang
Xi'an Research Institute of High Technology: PLA Rocket Force University of Engineering
jiangbo xu (xujiangbo@yeah.net)
Chang'an University School of Highway https://orcid.org/0000-0003-1567-0931
Baohua Cao
Chang'an University School of Highway
Danni Zhao
Chang'an University School of Highway
Wei Wei
Chang'an University School of Highway
Han Bao
Chang'an University School of Highway
Changgen Yan
Chang'an University School of Highway
Hengxing Lan
Institute of Geographic Sciences and Natural Resources Research CAS: Institute of Geographic Sciences and Natural Resources Research Chinese Academy of Sciences

Research Article

Keywords: Saturated remolded loess, Shear strength index, Dry density, Shear rate

Posted Date: July 2nd, 2021

DOI: https://doi.org/10.21203/rs.3.rs-156405/v2

Experimental study on shear strength of saturated remolded loess

Jie Lai[1], Yun Liu[1], Yuzhou Xiang[2], Wei Wang[1], Jiangbo Xu[3], Baohua Cao[3], Danni Zhao[3], Wei Wei[3], Han Bao[3], Changgen Yan[3], Hengxing Lan[4]

1. Xi'An Research Institute of High-tech, Xi'an 710025;
2. Chongqing Chengtou Road and Bridge Administration Co., Ltd, Chongqing 400015
3.Chang'an Unversity School of Highway, Xi'an 710064;
4. Institute of Geographic Sciences and Natural Resources Research, Beijing 100101;

Abstract: Loess has the characteristic of macropore, loose structure, homogeneous composition and collapsibility. It is easy to saturate when it encounters heavy rainfall and irrigation, resulting in landslides, roadbed subsidence and dam instability in the loess area. To study the influence of dry density and shear rate on shear strength of saturated remolded loess, an SLB-6A stress-strain controlled triaxial shear penetration tester was used to conduct Consolidated Undrained(*CU*) test in the Yan'an area. During the test, three variables of shear rate, confining pressure and dry density were controlled. The dry densities of the samples were 1.5g/cm^3, 1.6g/cm^3 and 1.7g/cm^3 respectively. The *CU* test of the saturated remolded loess at a confining pressure of 100*kPa*, 150*kPa*, and 200*kPa* was performed at a shear rate of 0.04*mm/min*, 0.08*mm/min*, 0.16 *mm/min*, and 0.4*mm/min* respectively. It is found that the stress-strain curve of saturated remolded loess gradually moves up with the increase of dry density. When the dry density is equal to ρ_d=1.5g/cm^3, the deviatoric stress under different confining pressures there is a tendency to increase first and then decrease with increases of shear rate. When the dry density is equal to ρ_d=1.6g/cm^3 and ρ_d=1.7g/cm^3, the deviational stress under different confining pressures shows the trend of increasing first, decreasing and then increasing with the increase of shear rate, which is different from that at the dry density ρ_d =1.5g/cm^3 at a shear rate v=0.4*mm/min*. When the dry density ρ_d=1.5g/cm^3, the cohesive force decreases first and then increases with the increase of shear rate. When the dry density ρ_d=1.6g/cm^3 and ρ_d=1.7g/cm^3, the cohesive force first increases at 0.08 mm/min, and then decreases with the increase of shear rate. The cohesion and internal friction angles tend to increase as the dry density increases.

Key words: Saturated remolded loess, Shear strength index, Dry density, Shear rate

0 Introduction

Loess is widely distributed in northwestern China, forming a loess area in Gansu, Shaanxi, Shanxi and other provinces are shown in Fig.1. In recent years, with the development of the national economy in the western loess region, large-scale leveling the mountain to build land and subgrade engineering project have increased dramatically. Due to its unique engineering properties, loess has caused landslides, dam instability (Xu et al., 2019), and roadbed collapsibility. The most serious geological disasters in the northwest region pose a serious threat to the safety of people's lives and property (Xu et al., 2019). Water infiltration and fine-grained soil backfilling lead to cracks on the road shoulder (Sun et al., 2019). For example, large-scale agricultural irrigation has led to the frequent occurrence of loess landslides (Ma et al., 2018). The influence of rainfall intensity on landslide was analyzed to build a rainfall threshold model (Wu et al., 2015). The improved frequency ratio method is used to evaluate the sensitivity of landslides (Li et al., 2017). Sensitivity analysis is conducted on the landslide stability of Xiaojiang watershed in Yunnan Province (Lan et al., 2002), and a new landslide analysis model is proposed based on GIS (Lan et al., 2003). Zizhou County of Yulin City is a typical loess plateau. According to the survey, there are 128 geological disasters in the county, including 78 landslides and 44 collapses (Li et al., 2014). Therefore, based on laboratory tests, the influence of various factors on the shear strength of saturated remolded loess is discussed, which is of great significance for revealing the mechanism of geological hazard induced by loess saturation.

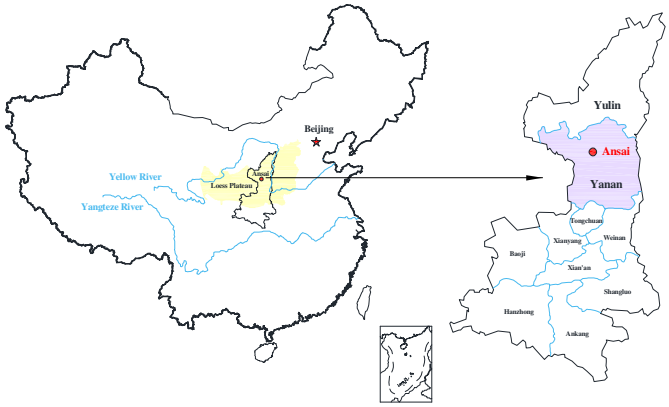

Fig. 1. Distribution of loess in China

At present, many scholars have carried out corresponding research on the influencing factors of the shear strength of loess and have made some achievements. The shear resistance of the contact between particles and the bite of the particles are important reasons for the shear resistance of the soil in the deformation (Lambe et al., 1969. the effect of bulk density and matrix potential on the shear strength of soil was studied (Cruse et al., 1977). Soil shear strength is defined as the resistance to a shear failure caused by continuous shearing of soil particles or soil masses (Kok et al., 1990). The combination of cohesive binding factors of clay and organic matter in soil subjected to varying wetting conditions exert a strong influence on the resistance of the soil to sustained shearing stresses (Al-Durrah et al., 1981). The influencing factors of soil shear strength after rainfall is studied (Watson et al., 1986). The relationship between the soil-water characteristic curve and the shear strength of unsaturated soil is described, which is related to matrix suction (Vanapalli et al., 1996). Am empirical, analytical model is developed to predict the shear strength in terms of soil suction. In the field of unsaturated soil research, The expression of effective stress of unsaturated soil similar to the principle of effective stress of Terzaghi, and extend the criterion of shear strength of saturated soil to unsaturated soil (Bishop et al., 1960). The shear strength formula is raised for unsaturated soils. Considering the influence of suction on the strength of unsaturated soils, and two different parameters were selected. The difficulty of the shear strength formula proposed by the above two scholars is that the effective stress parameter χ and the suction internal friction parameter φ_b are uncertain, which limits the practical application (Fredlund et al., 1978). Based on the consideration of the interaction between micro-particles and the effective stress of Terzaghi, and the theory of soil stress is proposed, which clarified the physical meaning of soil cohesion from the microscopic point of view, that is, the frictional strength generated by the suction stress in the soil during the shearing process (Ning et al., 2014). Influence of the history of shear paths on yield and failure surfaces is discussed, and the position of yield was found to be independent of the previous shearing path history of the soil and occurred at points that corresponded to a yield surface defined for the current shearing path direction (Malanraki et al., 2011). A hyperbolic function model based on the experimental data is advanced, which enriched the theoretical system of nonlinear shear strength function (Amaechi et al., 2015). The steady strength of saturated loess is studied under the stress-controlled undrained consolidation triaxial =tests . There are two typical stress-strain behaviors of saturated loess: steady-state behavior and quasi-steady state. In the majority of situations, it exhibits steady- state behavior. Only loose loess exhibits quasi-steady -state behavior (Zhou et al., 2010). The water migration in loess samples is researched based on the damage of water in subgrade (Yan et al., 2018). Soil samples of loess slope arecollected in Longdong, and carried out the shear test. It was found that the anisotropy of loess had little effect on friction angle, and had a certain effect on cohesion (Shi et al., 2019). an experimental study is presented to investigate the influence of sand and water content on the small-strain shear modulus (G_0) of Yan'an loess, and found that the roundness of soil particles can reduce the shear wave velocity (Liu et al., 2019). Strain softening exists in fault gouge as well as loess through the cyclic shear test (Bao et al., 2019). The effects of dry density on the strength and deformation characteristics of Q_2 remolded loess is analyzed. The test results show

that the deviatoric stress-axial strain curves of the specimens are strain hardened under different dry densities. As the dry density increases, the deviatoric stress of the sample increases remarkably, and the hardening tendency increases gradually (Zhang et al., 2019). Quantitative parameters are raised to reflect the structure of remolded loess and undisturbed saturated loess based on the triaxial test (Chen et al., 2010). *UU* and *CU* tests on saturated undisturbed loess are carried out, and obtained the relationship between the initial tangential modulus, shear strength and stress path of the undisturbed loess under different confining pressures (Yang, 2007). (Leng, 2014) considered the influence of confining pressure on the shear strength of saturated loess and gave the corresponding strength reduction formula. Saturated loess with different dry density through different stress paths are researched, and found that under the same path, the stress-strain, the size of dry density does not affect the shape of its curve, but the strength and anti-destructive ability of the soil (Jiang, 2010). The modified TFB-1 unsaturated soil stress-strain control triaxial apparatus is used to carry out saturation test and *CU* test on the remolded soil samples of Malan loess in the Dangchuan area, and the study found that the shear strength of saturation remolded loess under the same confining pressure increases first and then decreases with the increase of shear rate. Under the same shear rate, the shear strength of saturated remolded loess increases with the increase of confining pressure. CTC and RTC tests are conducted on saturated remolded loess and saturated undisturbed loess, and it is found that the shear strength of saturated undisturbed loess under low confining pressure is higher than that of saturated remolded loess, and the opposite under high confining pressure (Jiang, et al., 2011).

In summary, scholars at home and abroad have carried out some research on remolding saturated loess, and have achieved corresponding results in shear rate and confining pressure on the shear strength of loess. However, the study on the influence of various factors on the shear strength of loess is still in the preliminary stage of exploration in laboratory tests, and no systematic theoretical system has been formed. It is difficult to obtain the undisturbed loess in reality, so laboratory tests are carried out on remolded loess in the Yan'an area. First, water head saturation and back pressure saturation are used to saturate the sample, and then the *CU* test is carried out directly on the sample. It is of practical significance and theoretical value to study the influence of various factors on the shear strength of remolded loess by combining the method of water head saturation, back pressure saturation and CU tests.

1 Soil sample and testing methodology

1.1 Materials

The test soil was a brownish -yellow silty clay and taken from the Ansai area of Yan'an, Shaanxi Province. Before the preparation of the test soil sample, the loess is first naturally dried and crushed, then screened by a 2 *mm* sieve and stored in a glass tank for reserve. Its physical properties are shown in Table 1. The granular gradation curve of the soil is shown in Fig.2. The size of the remolded soil sample in this test was 39.1*mm* × 80*mm*, wherein the sample diameter was 39.1*mm*, and the sample height was 80*mm*.

Table 1. Basic physical parameters of soil samples

Moisture content/%	Dry density/(*g* / $cm^{3)}$	Relative density of soil particles G_S	Percentage of soil particles at different particle sizes/%			
			< 0.075	0.075-0.25	0.25-0.5	0.5-2
14.97	1.557	2.71	88.73	12.27	0	0

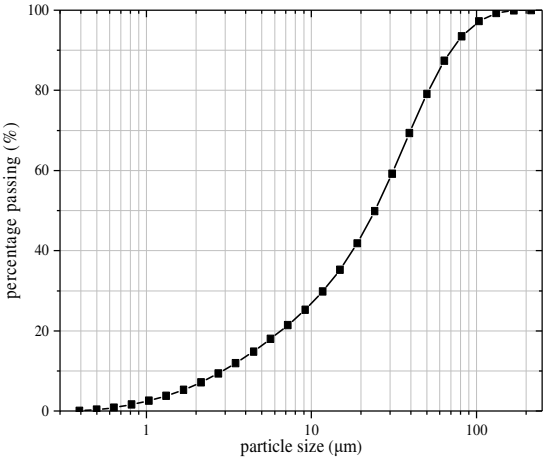

Fig. 2. Granular gradation curve of loess

1.2 Experimental method

The device used in this test is an SLB-6A stress-strain controlled triaxial shear permeability tester. Its confining pressure range is 0-1*MPa*, and the strain of clay is 0.05%-0.1% per minute. It can be controlled and collected data by computer. The test process is divided into three stages: water head saturation stage, back pressure saturation stage and *CU* stage. Firstly, 10*kPa* confining pressure is set to saturate the loess sample, and the air in the rubber film is discharged, the first confining pressure and back pressure are applied after the water head saturation is over to conduct the back pressure saturation, and each stage is increased by 10*kPa*. In the whole saturation test process, the water head saturation time is 3-4 hours and the back pressure saturation time is 5-6 hours, which greatly shortens the saturation time and the saturation effect is obvious. At the end of the saturation test, the B value is tested, that is, the back pressure remains unchanged, and the confining pressure is increased by 40*kPa*. The increment of pore water pressure caused by the increment of confining pressure $(\Delta\sigma_3)$ is Δu.

$$B = \Delta u/\Delta\sigma_3 \qquad (2)$$

It is difficult to achieve 100% B value in the actual test process. When the B value reaches 95%, it can be considered that the sample is saturated, and the back pressure valve is closed after the saturation test meets the test requirements.(The reasons are as follows. According to the results of triaxial compression tests, the relationship between the pore pressure and the large and small principal stresses under axisymmetric stress can be established by referring to the pore pressure coefficients A and B. By the effective stress formula and the elastic theory, when the elastic material elastic modulus and poisson's ratio of E and μ, in the equal to the stress, shear stress, the change of the soil volume formula can draw $B = \frac{1}{1+n\frac{Cv}{Cs}}$, where n represents the porosity of soil, C_v represent three to pore volume compressibility, C_s on behalf of the three to the volume compression coefficient of soil skeleton.Reason for saturated soil, completely filled with water in the pores, due to the compressibility of water is much lower than the compressibility of soil skeleton, $\frac{Cv}{Cs} \longrightarrow 0$, and B = 1; For dry soil, $\frac{Cv}{Cs} \rightarrow \infty$, therefore, B = 0; For unsaturated soil, 0<B<1 ,the less saturated the soil, the smaller the B value.) The dry density of the sample was determined as 1.5g/cm^3, 1.6g/cm^3 and 1.7g/cm^3. The CU test was carried out under the confining pressure of 100*kPa*, 150*kPa* and 200*kPa*, and the shear rate of 0.04*mm/min*, 0.08*mm/min*, 0.16*mm/min* and 0.4*mm/min* respectively. By controlling the shear rate and confining pressure, the relationships between dry density and cohesion, dry density and internal friction angle, shear rate and cohesion, shear rate and internal friction angle can be obtained respectively. The test plan is shown in Table 2 below.

Table 2. Test design scheme

Dry density/(g/cm^3)	Confining pressure/*kPa*	Shear rate/$mm \cdot min^{-1}$

1.5	100、150、200	0.04、0.08、0.16、0.4
1.6	100、150、200	0.04、0.08、0.16、0.4
1.7	100、150、200	0.04、0.08、0.16、0.4

3 Analysis of test results

Pore water pressure and axial strain are expressed by u and ε respectively, where p is the center coordinate of the circle of molar stress, q is the radius of the circle of molar stress, and σ_1 and σ_3 are the major and minor principal stresses respectively. The values of p and q are shown in Table 3.

$$p=（\sigma_1+\sigma_3）/2 \quad （3）$$

$$p'=（\sigma_1+\sigma_3）*0.5-u \quad （4）$$

$$q'=q=(\sigma_1-\sigma_3)/2 \quad （5）$$

Table 3. *p*&*p'*and *q* values at different dry densities and shear rates

Dry density/($g•cm^{-3}$)	Shear rate v/$mm•min^{-1}$	Confining pressure/*kPa*	*p*	*q*&*q'*	*p'*
1.5	0.04	100	146.20	46.20	67.20
		150	222.80	72.80	102.80
		200	284.80	84.80	115.80
	0.08	100	167.65	67.65	95.65
		150	231.80	81.80	99.80
		200	284.40	84.40	125.40
	0.16	100	146.25	46.25	67.25
		150	214.10	64.10	96.10
		200	294.20	94.20	122.20
	0.4	100	141.10	41.10	63.10
		150	207.65	57.65	82.65
		200	291.20	91.20	120.20
1.6	0.04	100	165.80	65.80	102.80
		150	241.55	91.55	131.55
		200	329.25	129.25	172.25
	0.08	100	217.25	117.25	145.25
		150	299.55	149.55	187.55
		200	370.00	170.00	214.00
	0.16	100	170.10	70.10	111.10
		150	226.25	76.25	122.25
		200	302.80	102.80	149.80
	0.4	100	203.95	103.95	132.95
		150	295.00	145.00	166.00
		200	347.95	147.95	197.95
1.7	0.04	100	222.45	122.45	176.45
		150	276.60	126.60	206.60
		200	394.80	194.80	281.80
	0.08	100	276.75	176.75	234.75
		150	346.55	196.55	278.55

		200	417.10	217.10	330.10
	0.16	100	216.95	116.95	175.95
		150	302.85	152.85	225.85
		200	364.25	164.25	247.25
	0.4	100	260.15	160.15	220.15
		150	338.10	188.10	275.10
		200	401.05	201.05	283.05

3.1 Effect of dry density and shear rate on deviation stress

Fig. 3~Fig. 5 is the stress-strain diagram of saturated remolded loess under different dry densities and shear rates. It can be seen that the deviatoric stress of the sample increases significantly at the same shear rate with the increase of dry density. The deviatoric stress-axial strain curves of the sample when ρ_d=1.7g/cm^3 are strain hardening. When ρ_d=1.5g/cm^3 and ρ_d=1.6g/cm^3, the deviatoric stress-axial strain curves of soil samples show two forms: weak softening and softening, and the softening is obvious under low confining pressure. Generally, the peak value of σ_1-σ_3 is taken as the failure point, but the deviatoric stress at 15% axial strain is taken as the failure point when there is no peak value. The deviatoric stress- axial strain curve of saturated remolded loess can be divided into two stages. In the first stage, the deviatoric stress rapidly reaches the peak point with the strain increase, and then enters the second stage. The deviatoric stress tends to decrease slowly with the increase of strain, and approaches a certain value when the strain reaches 20%, which is no obvious stress drop in the whole stage.

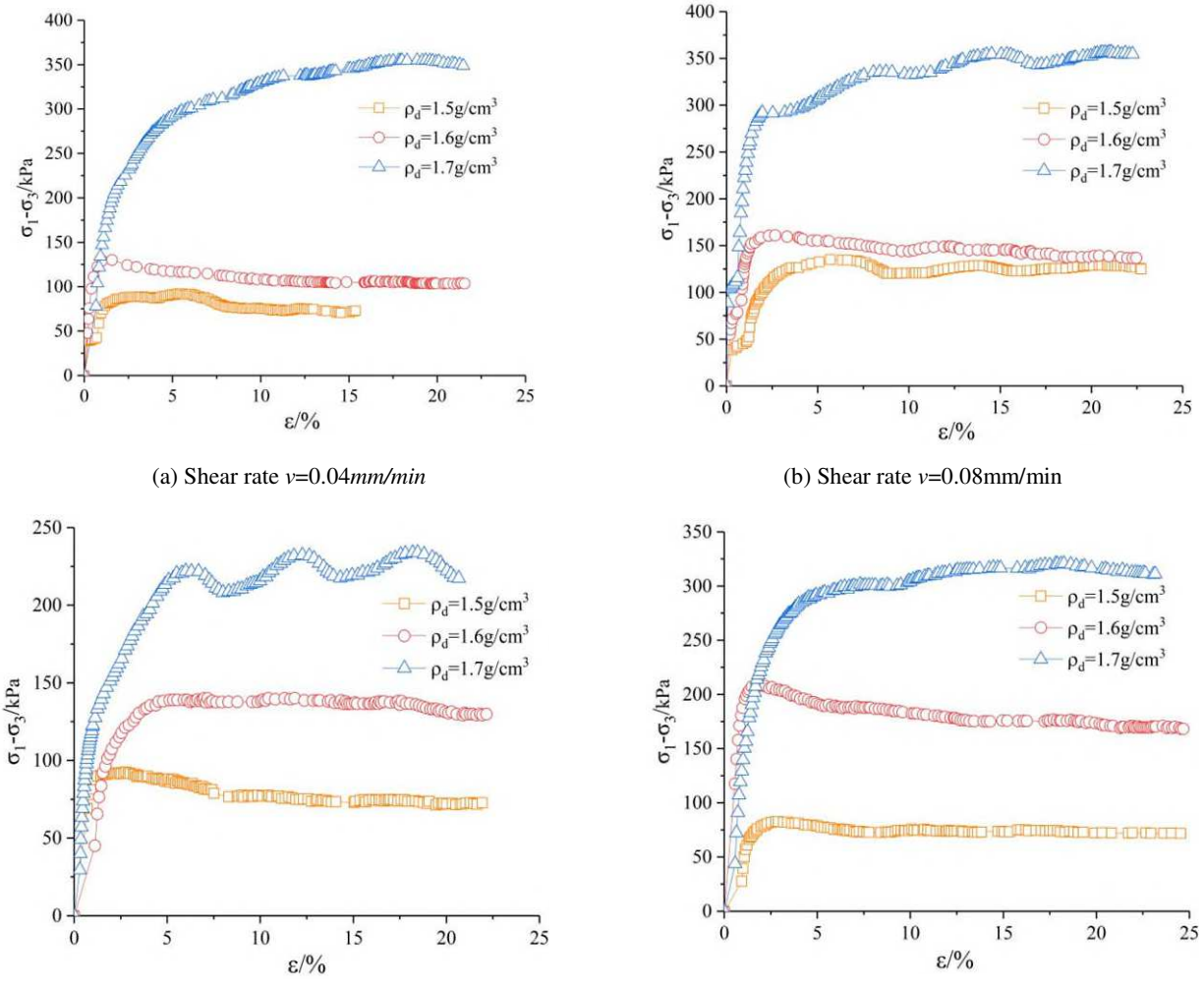

(a) Shear rate v=0.04mm/min (b) Shear rate v=0.08mm/min

(c) Shear rate v=0.16mm/min (d) Shear rate v=0.4mm/min

Fig. 3. σ_1-σ_3~ε curve under confining pressure of 100kPa

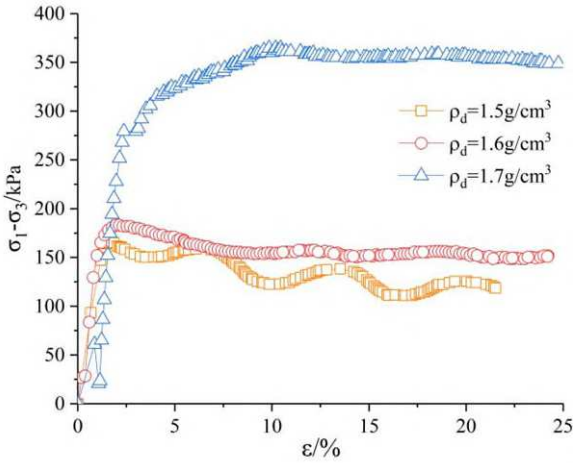

(a) Shear rate *v*=0.04*mm/min*

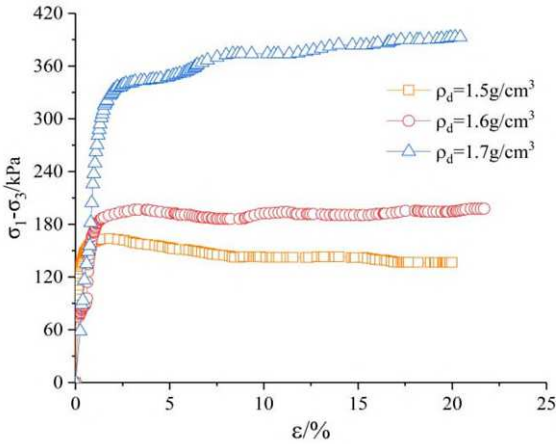

(b) Shear rate *v*=0.08*mm/min*

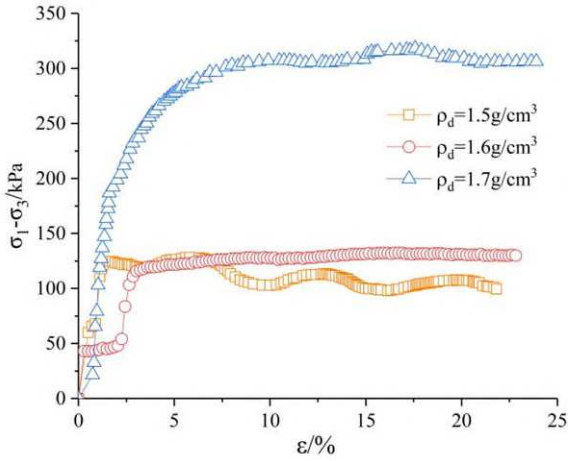

(c) Shear rate *v*=0.16*mm/min*

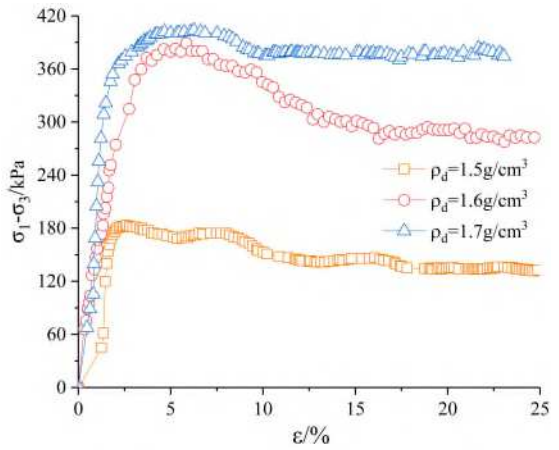

(d) Shear rate *v*=0.4*mm/min*

Fig. 4. σ_1-σ_3~ε curve under confining pressure of 150*kPa*

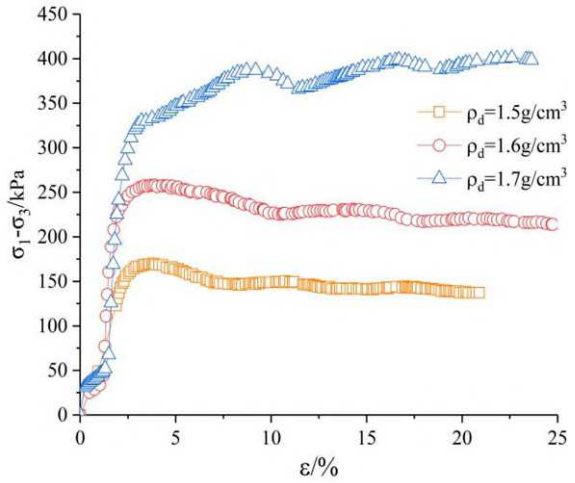

(a) Shear rate *v*=0.04*mm/min*

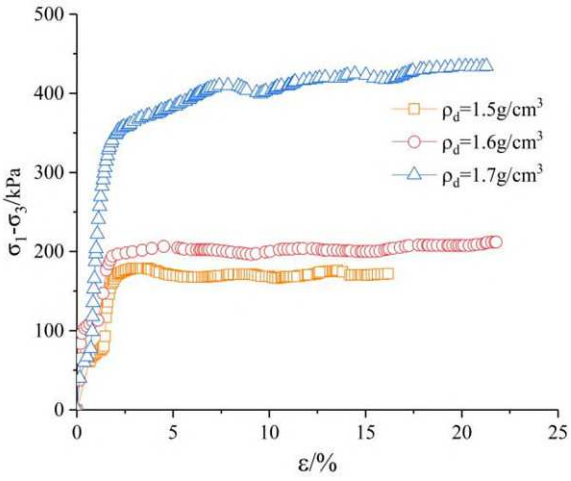

(b) Shear rate *v*=0.08*mm/min*

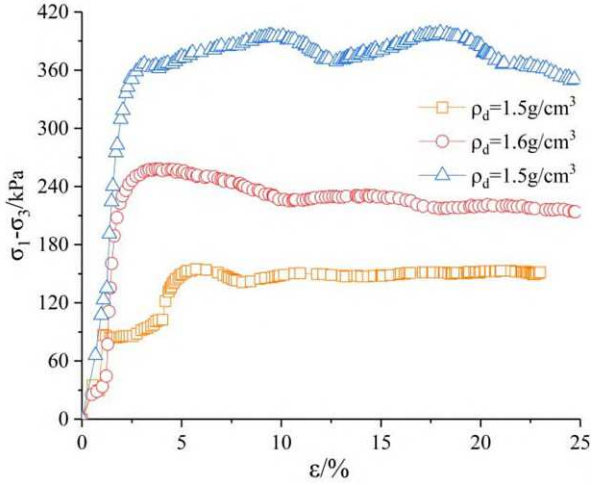

(c) Shear rate v=0.16*mm/min*

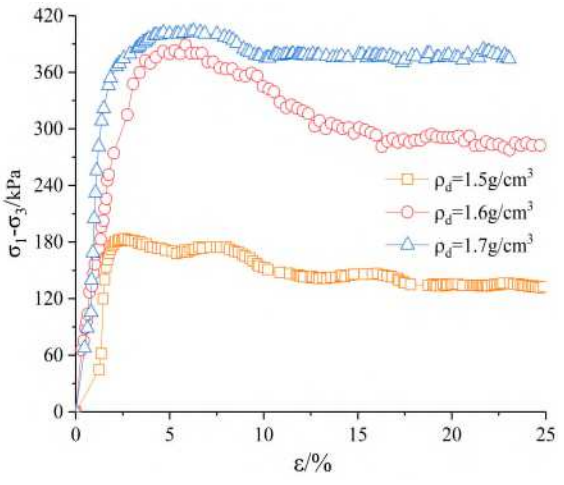

(d) Shear rate v=0.4*mm/min*

Fig. 5. σ_1-σ_3~ε curve under confining pressure of 200*kPa*

It is the curve of pore water pressure versus strain from Fig. 6. When the soil sample reaches a saturation state, the free water fills the whole soil pore. Because water can not be compressed and does not bear shear force, it exists between soil particles as a barrier zone, which affects the contact between particles. Most of its occlusive friction is offset by the lubrication of pore water, which reduces the cohesion between soil particles and increases the irrecoverable plastic strain in the sample, and finally make the strength reduce. The larger the dry density, the less the pores of the soil, and the free water in the pores is relatively reduced, so the less the occlusive friction between the soil particles is offset, the relatively strong the shear strength during shearing. When the dry density value is high, the soil sample is in a dense state, and the peak value of the deviatoric stress-axial strain curve is large, while the pore water pressure tends to appear negative pore water pressure, showing a large dilatancy, and thus a lower pore water pressure.

With the shear rate as the transverse axis and the peak point of deviatoric stress under the same confining pressure or the deviatoric stress corresponding to 15% axial strain as the longitudinal axis to require the relationship curve between the deviatoric stress and the shear rate under different confining pressures, which is drawn from Fig. 7. It can be seen that the shear strength of saturated remolded loess under the same confining pressures obviously affected by the shear rate, and the relationship between the shear strength and the shear rate is not a simple monotone function. It is generally believed that the deviatoric stress increases with the increase of strain rate, which is different from the experimental results. When the dry density is ρ_d=1.5*g/cm*^{3}, it can be shown from Fig. 7(a) that the shear strength increases first and then decreases as the shear rate increases, and there is a significant critical shear rate. As the confining pressure increases, the overall appearance increases and then decreases. The softening behavior at a high strain rate is significantly higher than that at a low strain rate. This phenomenon may be related to the thixotropy of loess. The loess clay structure of the high strain rate may be destroyed, which may lead to the softening phenomenon called strain rate softening. When the shear rate is low, the loess structure is not obviously damaged, and the partial strength of the loess loss can be recovered. At the higher shear rate, the loess structure is destroyed, and the strength of loss is relatively large, which leads to the appearance of low shear strength at a high shear rate (Chen et al., 2010). When the dry density is equal to ρ_d=1.6*g/cm*^{3} and ρ_d=1.7*g/cm*^{3}, it can be revealed from Fig. 7(b) and Fig. 7 (c) that as the shear rate increases, the deviatoric stress has the trend of increasing first, decreasing and then increasing with the shear rate. It can be inferred that when the shear rate is small, the structural properties of loess are not destroyed and some strength of loess can be restored, but the internal clay of loess tends to be destroyed when the test is about 0.16*mm/min*, and the strength of loess recovers slowly, so there is a downward trend. The permeability coefficient of loess decreases relatively when the dry density is relatively large, and uneven pore pressure will occur at an excessively high shear

rate, which limits the selection range of shear rate, thus the thixotropy of loess can not be expressed. The effect of shear rate on the shear strength of loess is also the result of a combination of many factors. The strain -softening phenomenon is weaker in soils with relatively low thixotropy, and the shear strength increases with the increase of strain rate. When the dry density is large, the strength of saturated loess increases relatively with time in the shear process. As a result, with the increase of shear rate, the thixotropy of loess did not make the structural properties of loess be damaged obviously, and the partial strength of loess could be restored quickly. Thus, the deviatoric stress increased with the increase of shear rate between 0.16*mm/min* and 0.4*mm/min*.

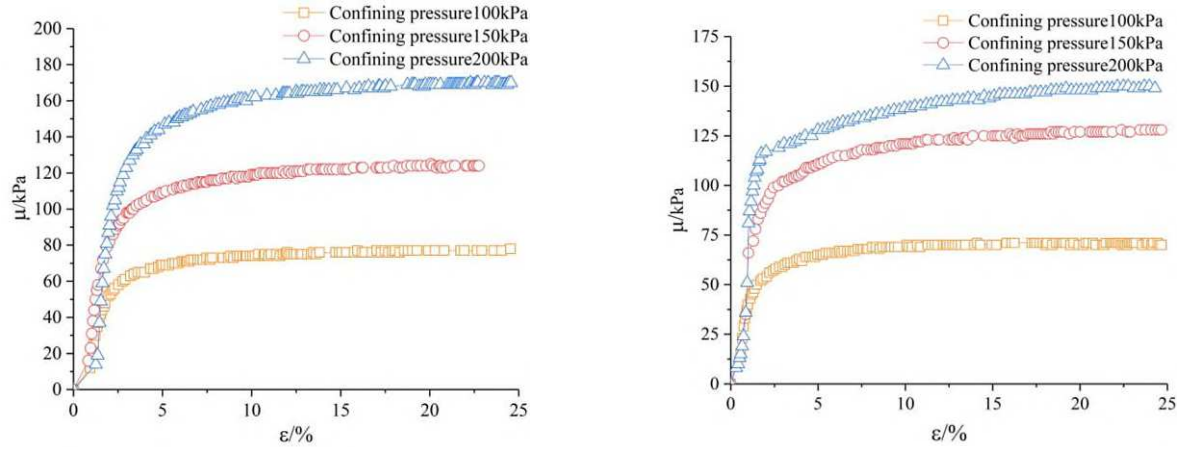

(a) ρ_d=1.5*g/cm*^{3} (b) ρ_d=1.6*g/cm*^{3}

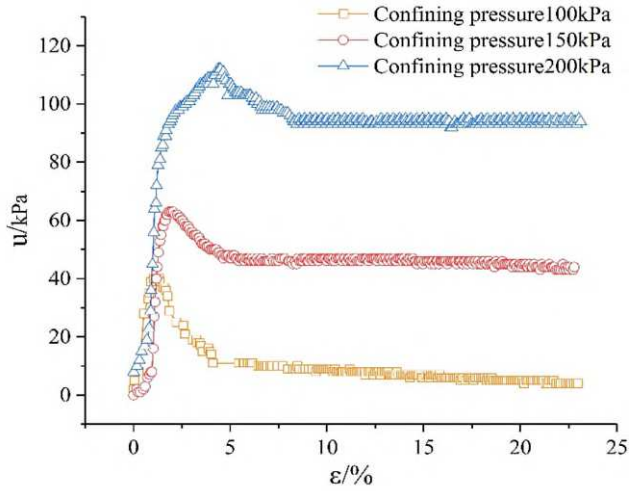

(c) ρ_d=1.7*g/cm*^{3}

Fig. 6. Pore water pressure *u* curve with shear rate of 0.4mm/min at dry density of 1.5g/cm^3, 1.6g/cm^3, 1.7g/cm^3

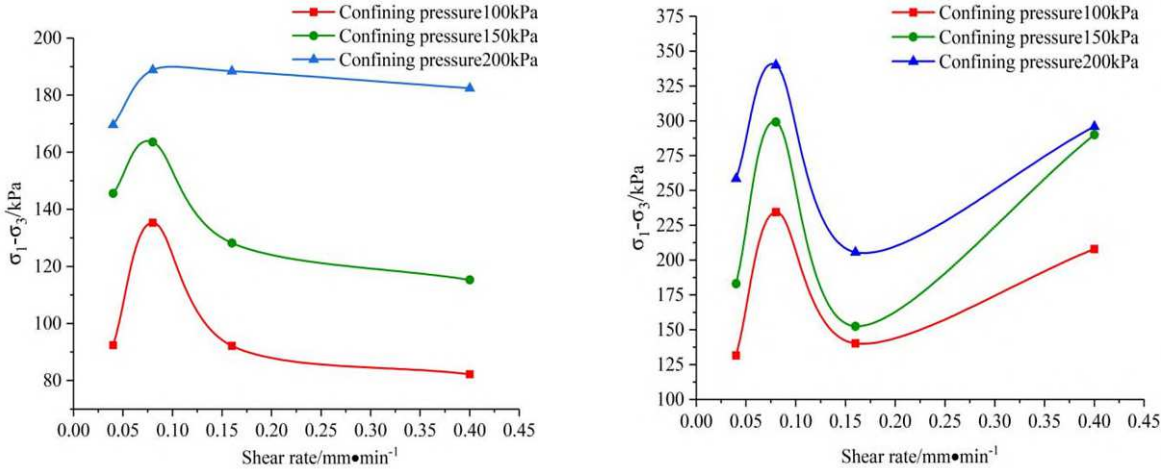

(a) ρ_d=1.5g/cm^3 (b) ρ_d=1.6g/cm^3

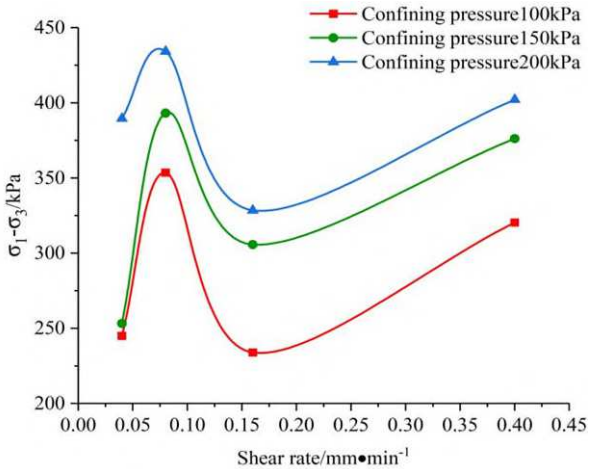

(c) ρ_d=1.7g/cm^3

Fig. 7. The Relation between deviatoric stress and shear rate under different confining pressures

3.2 Effect of shear rate and dry density on stress path

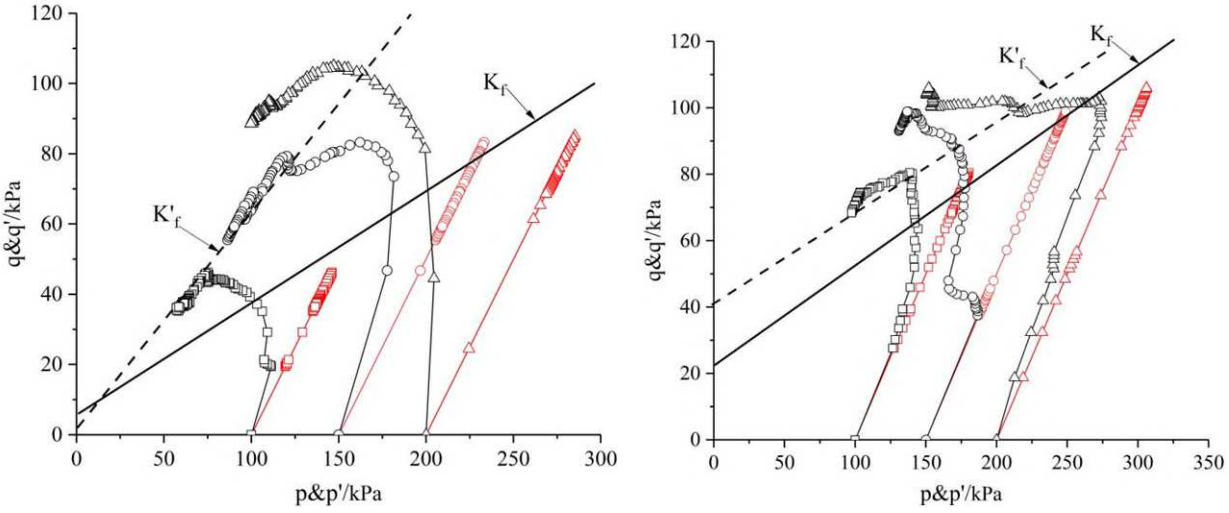

(a) Shear rate v=0.04mm/min (b) Shear rate 0.04mm/min

Fig. 8. p~q curve with ρ_d=1.5g/cm^3 and ρ_d=1.6g/cm^3

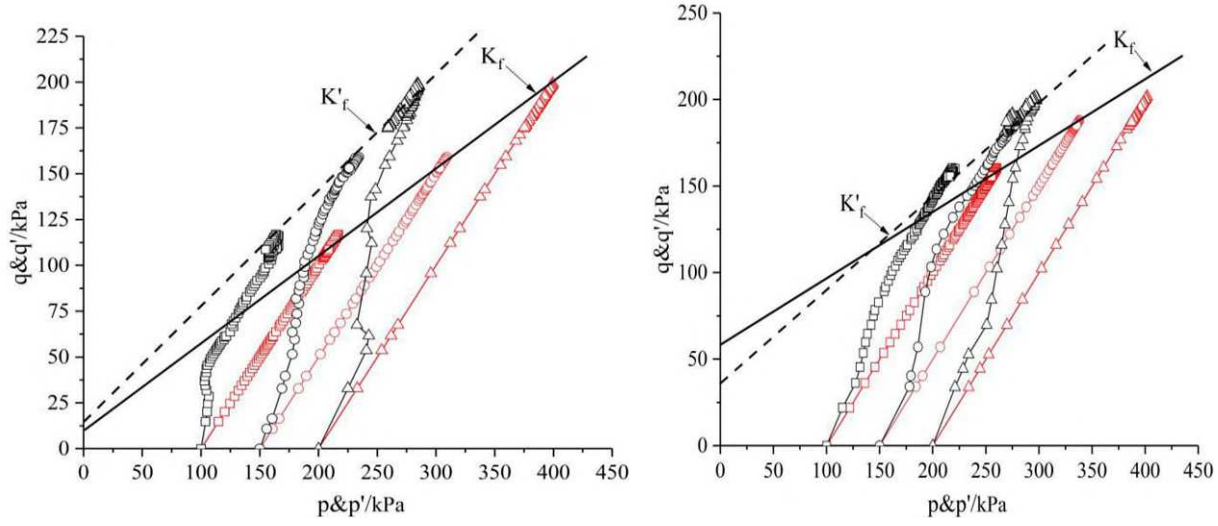

(a) Shear rate v=0.16mm/min (b) Shear rate v=0.4mm/min

Fig. 9. p~q curve with ρ_d=1.7g/cm^3

Fig. 8(a), (b), Fig. 9(a), (b) are the p~q and p'~q curves of saturated remolded loess under confining pressure of 100kPa, 150kPa and 200kPa respectively. The failure principal stress lines K'_f of effective stress path and failure principal stress lines K_f of total stress path are the aggregation of all the points in limit equilibrium stress state to show in p'-q coordinate system and p-q coordinate system respectively. In this paper, only a few representative graphs are selected. When undrained shear occurs, the deviatoric stress σ_1-σ_3 is increased, and the total stress path develops upward in a straight line with a certain angle to the p-axis until the soil sample is destroyed. Excess pore water pressure u is generated in the specimen during undrained shear. The pore pressure coefficient A changes continuously during shear for saturated soil, and the effective stress path is a curve.

$$u = A \times (\sigma_1 - \sigma_3) \quad (6)$$

$$p' = p - u \quad (7)$$

The undrained shear stress path of saturated remolded loess under low confining pressure is obviously different from that under high confining pressure. The effect of larger dry density on the stress path of saturated remolded loess is greater than that of lower dry density. As shown in Fig. 9 (a), (b), the shapes of the curves are different under different shear rates. With the increase of confining pressure, the initial stage of the stress path is more and more perpendicular to the p-axis. With the increase of strain, the stress path first reaches its peak strength at different shear rates, and then tends to a narrow region in the stress space. This phenomenon shows that the concept of critical state is still applicable to remolded loess related to shear rate.

3.3 Variation of shear strength index with shear rate and dry density

The values of total residual strength parameters c, φ and effective residual strength parameters c', φ' of the saturated remolded loess in CU test can be obtained by linear fitting of p~q and p'~q curves. The intercept between the fitting line and the ordinate is c_q, and the slope is φ_q. There is a relational expression between c_q, φ_q and cohesion c, friction angle φ(8), (9), and the total residual shear strength index and effective residual shear strength index of saturated remolded loess at different shear rates are shown in Table 4.

$$\sin\varphi = \tan\varphi_q; \quad (8)$$

$$c = c_q / \cos\varphi; \quad (9)$$

Table 4. Effective residual shear strength and total residual strength under different dry density and shear rate conditions

Dry density /(g•cm^{-3})	Shear rate/mm•min^{-1}	c/kPa	φ /(°)	c'/kPa	φ'/(°)
1.5	0.04	6.940	16.320	24.286	29.406
	0.08	6.199	17.999	23.451	33.025
	0.16	6.874	16.559	24.152	29.736
	0.4	8.562	15.308	24.358	28.164
1.6	0.04	12.778	20.121	28.174	31.870
	0.08	28.307	23.891	50.223	34.960
	0.16	7.395	18.844	17.148	32.480
	0.4	37.762	20.060	54.674	31.064
1.7	0.04	33.864	23.079	30.015	32.208
	0.08	40.877	27.580	42.653	35.170
	0.16	29.252	23.578	29.819	33.642
	0.4	55.076	23.453	55.101	31.668

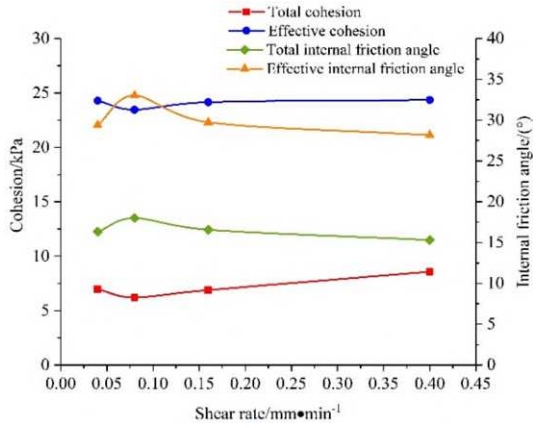

(a) ρ_d=1.5g/cm^3

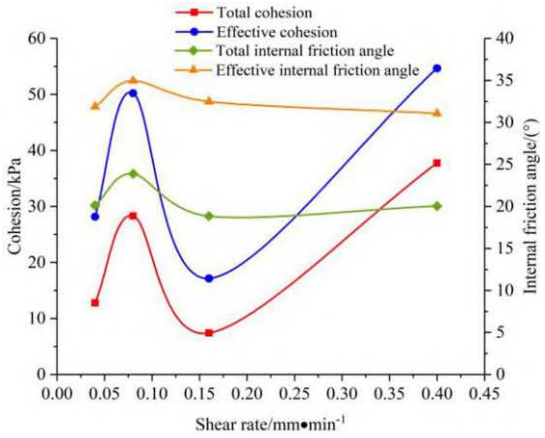

(b) ρ_d=1.6g/cm^3

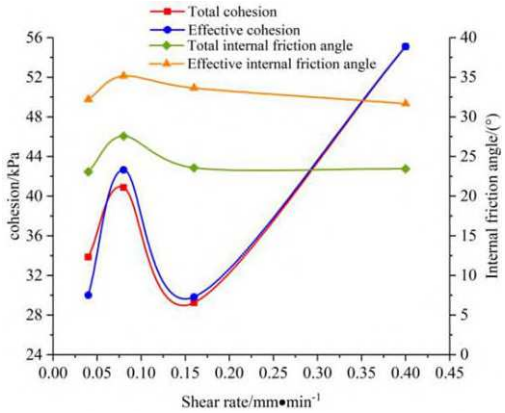

(c) ρ_d=1.7g/cm^3

Fig. 10. Relationship between cohesion, internal friction angle and a shear rate of saturated remolded soil samples

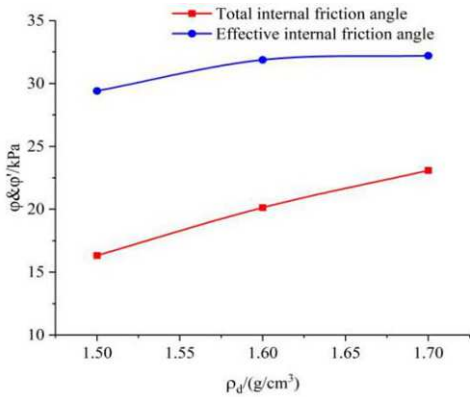

Fig. 11. The Curve of shear strength index *c* with dry density

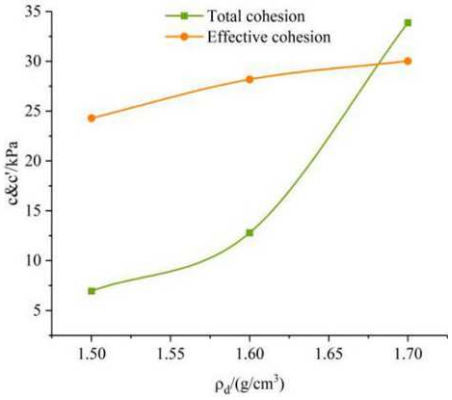

Fig. 12. The Curve of shear strength index *φ* with dry density

The shear rate is the horizontal axis, and the shear strength index of the saturated remolded loess sample is the vertical axis. The relationship between the cohesion, the internal friction angle of the remolded soil sample and the shear rate is plotted. As shown in Fig. 10 (a), (b), (c), the total and effective internal friction angles of saturated remolded loess under different dry densities, always increase first and then decreases with the increase of shear rate. When dry density is equal to 1.5*g/cm*^{3}, the cohesion decreases first and then increases with the increase of shear rate. When dry density is equal to 1.6*g/cm*^{3} and equal to 1.7*g/cm*^{3}, with the increase of shear rate, the cohesion first increases at 0.08*mm/min*, after that, the cohesive force decreases first and then increases. This phenomenon may be caused by swelling of saturated soil samples during the *CU* test. The cohesion of soil is composed of original cohesion and solidified cohesion. The former comes from the electrostatic force and van der

Waals force between particles, that is to say, it is determined by the gravity between particles molecules in the soil, which is related to the density of the soil. The latter depends on the cementation of cementitious materials between particles. The test soil sample is fine-grained silty loess, and the internal friction angle of the fine-grained soil is affected by density, particle gradation, particle shape, etc. The denser the soil, the smaller the roundness, the stronger the bite cooperation and the greater the internal friction angle (Li et al., 2018). During the *CU* test, the soil sample continued to dilate lead to the volume became larger, and the dry density became relatively smaller, which was the main reason for the change of the original cohesion and the internal friction angle.

The relationship between cohesion, internal friction angle of 0.04*mm/min* shear rate and dry density in Table 4 is shown in Fig. 11 and Fig. 12. From the graph, it can be seen that cohesion and internal friction angle of saturated remolded loess samples increase with the increase of dry density. Because of the larger density of the sample, the pores between the particles are gradually reduced due to compaction, and the particles are more closely contacted with each other, which causes the bite and the frictional force to increase accordingly between the particles, so the cohesive force increases significantly with the increase of dry density. As the dry density increases, the contact between the particles in the soil also tends to be tight, and the void ratio is relatively reduced. The moisture in the sample mostly remains in the manner of strongly binding the water film on the surface of the soil particles, and the strong absorbed water is relatively stable and cannot move, so the internal friction angle φ of the sample shows an increasing tendency as its dry density increases. The above shows that the internal friction angle does not increase infinitely with the increase of dry density, and there may be a critical value (Chen et al., 2005), while the cohesion increases with the increase of dry density.

4 Conclusion

(1) At the same shear rate, with the increase of dry density, the deviatoric stress of the specimens increases significantly. The deviatoric stress-axial strain curves of the specimens at different dry densities are strain-hardening, and the hardening trend of the specimens increases with the increase of dry density. The stress-strain curves of the saturated remolded soil specimens show two forms of weakening and softening under a certain shear rate, and the softening is obvious under low confining pressure.

(2) The shear strength of saturated remolded loess increases first and then decreases with the increase of shear rate and confining pressure when dry density is equal to ρ_d=1.5g/cm^3, which is an obvious critical strain rate. When dry density is equal to ρ_d=1.6g/cm^3 and ρ_d=1.7g/cm^3, the deviatoric stress increases first, then decreases andincreases with the increase of shear rate, which is different from that when dry density is equal to ρ_d=1.5g/cm^3 when the shear rate is 0.4*mm/min*.

(3) When dry density is equal to 1.5g/cm^3, the cohesion decreases first and then increases with the increase of shear rate. When dry density is equal to *1.6*g/cm^3 and 1.7g/cm^3, the cohesive force first increases at 0.08mm/min, and then decreases first and then increases with the increase of shear rate.

(4) With the increase of dry density, the cohesion and internal friction angle of remolded saturated loess samples has an increasing trend. When the dry density is small, the increasing trend of shear strength index φ is larger, but with the increase of dry density, the increasing trend slows down, while the cohesion raises with the increase of dry density as a whole.

Conflicts of Interest

The authors declare that there are no conflicts of interest regarding the publication of this paper.

Acknowledgements

This work was partially supported by the Fundamental Research Funds for the Central Universities, CHD (No.300102219213), Project Mechanism of mega loess slope sliding supported by NSFC (No.41790443), Key R&D Program of Shaanxi Province (2018ZDXM-SF-024).

References:

Al-Durrah, M., Bradford, J. M.. New methods of studying soil detachment due to waterdrop impact [J]. Soil Science Society of America Journal, 1981, 45(5): 949-953.

Amaechi J, Anyaegbunam. Nonlinear power-type failure laws for geomaterials: Synthesis from triaxial data, properties, and applications [J]. International Journal of Geomechanics, 2015, 15 (1):14-36.

Bao, H., Qi, Q., Lan H, et al, 2019. Shear Mechanical Behaviours and Multistrength Parameter Characteristics of Fault Gouge [J]. Advances in Civil Engineering. https://doi.org/10.1155/2019/4208032

Bishop, A.W., Alpin, L., Blight, G. E., et al. Factor Controlling the Shear Strength of Partly Saturated Cohesive [A]. Research Conference on the Shear Strength of Cohesive Soils[C]. University of Colorado, 1960:503-532.

Chen, T. L., Zhou, C., Shen, Z. J.. Experimental study on compression and shear properties of structural clay [J]. Chinese Journal of Geotechnical Engineering, 2005, 01(26):31-35.

Chen, H., Liu, M. Z., Song, Z. P.. Study on structural parameters of disturbed loess and saturated intact loess [J]. Chinese Journal of Underground Space and Engineering, 2010, 06(3):487-491.

Cruse, R. M., Larson, W. E.. Effect of soil shear strength on soil detachment due to raindrop impact [J]. Soil Science Society of America Journal, 1977, 41(4):777-781.

Fredlund, D. G., Morgenstern , R. A.. The Shear Strength of Unsaturated Soils [J]. Canadian Geotechnical Journal, 1978, 15:313-321.

Jiang, Y. M.. Study on the influence of stress path on the strength deformation and pore pressure characteristics of saturated loess [D]. Northwest A&F University, 2010.

Jiang, M., Hu, H., Peng, J., et al. Experimental study of two saturated natural soils and their saturated remolded soils under three consolidated undrained stress paths[J]. Frontiers of Architecture and Civil Engineering in China, 2011, 05(2):225-238.

Kok, H., McCool, D. K.. Quantifying freeze/thaw-induced variability of soil strength [J]. Transactions of the ASAE, 1990, 33(2):0501-0506.

Lan, H. X., Wu, F. Q., Zhou, C. H., et al. Sensitivity analysis of landslide factors in Xiaojiang watershed of Yunnan Province Based on GIS[J]. Chinese Journal of Rock Mechanics and Engineering, 2002, 21(10), 1500-1506.

Lan, H. X., Zhou, C. H., Wu F. Q., et al. Spatial analysis and prediction of rainfall-induced landslide risk supported by GSI [J]. Chinese Science Bulletin, 2003, 48(5):507-512.

Lambe, T. W., Whitman, R. V.. Soil mechanics [M], New York: John Wiley & Sons, 1969.

Leng, Y. Q.. Deformation strength characteristics of saturated-unsaturated remolded loess [D]. Chang'an University, 2014.

Li, L. P., Lan, H. X., Guo, C. B.. A modified frequency ratio method for landslide susceptibility assessment [J]. Landslides, 2017, 14 (2):01-15.

Li, J. J.. The risk evaluation study on the geological hazards in Zizhou county [D]. Xi'an University of Science and Technology, 2014.

Li, W., Zhuang, J. Q., Wang, Y.. Experimental study on influence factors of shear strength of saturated remolded loess [J]. Journal of Engineering Geology, 2018, 26(3):626-632.

Liu, X., Yang, J.. Shear wave velocity in the sand: effect of grain shape [J]. Géoechnique, 2018, 68(8):01–22.

Liu, X., Zhang, N., Lan, H. X. et al. Effects of sand and water contents on the small-strain shear modulus of loess [J]. Engineering Geology Engineering Geology, 2019, 260(3):105202.

Ma, P. H., Peng, J. B., Li, T. L., et al. Forming mechanism and motion characteristics of the "3 • 8" Jiang-Liu loess landslide in Jingyang county of Shaanxi province [J]. Journal of Engineering Geology, 2018, 26(3):663-672.

Malanraki, V., Toll, D. G.. Triaxial tests on weakly bonded soil with changes in stress [J]. Journal of Geotechnical and Geoenvironmental Engineering, 2001, 127(3):282-29.

Ning, L., Murat, K.. A power law for elastic moduli of unsaturated soil [J]. Journal of Geotechnical and Geoenvironmental Engineering, 2014, 140:46-56.

Shi, Y. L., Wang, R., Yuan, H., et al. Quantitative reinforcement analysis of loess slope with anisotropy [J]. Advances in civil engineering, 2019(3):1-12.

Sun, W. F., Yan, C. G., X.W., et al. Deformation of Geogrid-Reinforced Segmental Retaining Wall due to Insufficient Compaction of Loess Backfill: Case Study in Shaanxi Province, China. Journal of Performance of Constructed Facilities, 2019, 33(6): 04019071.